

Original research article

# Secondary metabolites from halotolerant filamentous fungi as potential topical cosmeceutical ingredients

Chi Hoang<sup>1,2</sup>, Ha Tran<sup>1</sup>, Hang Tran<sup>1,2</sup>, Diep Hoang<sup>3</sup>, Quan Nguyen<sup>1,2</sup>, Cuong Le<sup>1,2\*</sup>

<sup>1</sup> Institute of Natural Products Chemistry – Vietnam Academy of Science and Technology, Hanoi, Vietnam

<sup>2</sup> Graduate University of Science and Technology – Vietnam Academy of Science and Technology, Hanoi, Vietnam

<sup>3</sup> VNU University of Engineering and Technology, Hanoi, Vietnam

## Abstract

The use of natural products in cosmetics and pharmacy has risen dramatically in recent years, leading to the overexploitation of flora and fauna worldwide and threatening the environmental sustainability. Microbe-derived components could help to solve the problem due to their independently controllable cultural property. To investigate the potential of microfungi for producing potential novel cosmeceuticals, cerevisterol (1), aloesol (2), 3 $\beta$ ,5 $\alpha$ ,9 $\alpha$ -trihydroxyergosta-7,22-diene-6-one (3), and ergosterol peroxide (4) were isolated from the halotolerant fungal strains *Penicillium brefeldianum* CL6 and *Talaromyces* sp. S3-Rt-N3. They were then tested for biological properties, including anti-microbial, tyrosinase inhibitory, and wound healing activities. The results revealed the wound-healing potentials of two fungal compounds – (1) and (2) – in terms of cell proliferation promotion in NIH-3T3 murine fibroblasts, and the tyrosinase inhibitory potential of fungal compounds (1), (3), and (4) in the substrates L-tyrosine and L-3,4-dihydroxyphenylalanine (L-DOPA). Interestingly, compound (1) exhibited antimicrobial activity against acne-causing bacterium *Propionibacterium acnes*. These results have revealed new prospects for the application of microorganisms-derived compounds, especially in the cosmetics industry.

**Keywords:** Cosmeceutical; Ergosterol; Halotolerant; Tyrosinase inhibitor; Wound healing

## Highlights:

- Four compounds were isolated from halotolerant fungi *Penicillium* and *Talaromyces*.
- Of the four isolated compounds, three were found to be *in vitro* skin-whitening, one exhibited *in vitro* anti-acne activity, and two had wound-healing potential.
- Fungi-derived compounds could serve as potential materials for new skin caring agents.

## Introduction

The term ‘cosmeceutical’ was first proposed in 1962 as “a scientifically designed product intended for external application to the human body” (Reed, 1962), and later described as a category of cosmetic products with performance characteristics of pharmaceuticals (Kligman, 2000). Today, “cosmeceuticals” has become a field of study for the discovery and innovation of safe ingredients and formulations to be used in the beauty industry, predominantly skin care (Espinosa-Leal and Garcia-Lara, 2019). The recent explosive demand for natural skin care products to counteract deleterious external impacts, such as photo-damage, cutaneous wounds, dryness, and microbial infection, has led to the acceleration of exploiting biologically active ingredients from plants and animals for cosmeceutical purposes.

Cosmeceuticals of natural origin were believed to be more effective, innocuous, and causing less side effects (Espino-

sa-Leal and Garcia-Lara, 2019). Famous examples are terrestrial botanical phenolics, polyphenols, flavonoids, terpenoids, steroids (Dorni et al., 2017) and marine organisms’ phlorotannins (Sanjeeva et al., 2016), polysaccharides, and carotenoid pigments (Corinaldesi et al., 2017). Recently, fungi have emerged as an alternative and relatively untapped source of cosmeceuticals for skin ageing and depigmentation applications (Agrawal et al., 2018). Besides, these microbes are able to be cultivated and fermented independently *in vitro* using laboratory-controlled environments, therefore could prevent the ecosystem from the scenario of resources depletion in large-scale consumption and over-exploitation.

Many fungi-derived metabolites were known to exhibit diverse skin cosmeceutical properties, including photo-protection, skin-whitening, anti-acne, and wound-healing activities. Since microfungi are among the most affected living organisms by global warming and increasing solar radiation, they were proposed to develop various adaptive strategies, including the induction of sporulation and the synthesis of photo-protective

\* **Corresponding author:** Cuong Le, Institute of Natural Products Chemistry - Vietnam Academy of Science and Technology, 1H building, 18 Hoang Quoc Viet, Cau Giay, Hanoi, Vietnam; e-mail: [lehcuong@yahoo.com](mailto:lehcuong@yahoo.com)  
<http://doi.org/10.32725/jab.2025.013>

Submitted: 2023-12-29 • Accepted: 2025-09-18 • Prepublished online: 2025-09-23

J Appl Biomed 23/3: 152–162 • EISSN 1214-0287 • ISSN 1214-021X

© 2025 The Authors. Published by University of South Bohemia in České Budějovice, Faculty of Health and Social Sciences.

This is an open access article under the CC BY-NC-ND license.

pigments, to protect themselves against ultraviolet challenges (Wong et al., 2019). Of all the fungal compounds involved in UV-tolerances, melanin, carotenoids, and mycosporines are the most described molecules (Nosanchuk et al., 2015; Wong et al., 2019). Hundreds of UV-absorbing mycosporins producers have already been documented, comprising selected fungal strains belonging to genera *Ascochyta*, *Aureobasidium*, *Cladosporium*, *Coniosporium*, *Cryptococcus*, *Phaeococcus*, *Rhodotorula*, *Sarcinomyces*, *Trichothecium*, and *Xanthophyllomyces* (Görünmek et al., 2024; Kogej et al., 2006; Libkind et al., 2011; Moliné et al., 2011; Volkmann and Gorbushina, 2006).

Carotenoids from isolates of genera *Rhodotorula*, *Phaffia*, and *Xanthophyllomyces* were claimed to possess anti-oxidant and anti-inflammatory activities that can contribute to photo-protection (Agrawal et al., 2018; Galasso et al., 2017; Kogej et al., 2006). Likewise, the existence of melanin was considered an effective armor in mycelia against photo-damage, with wide distribution in fungal clades of *Aspergillus*, *Fonsecaea*, *Neurospora*, *Sporothrix*, *Wangiella*, *Verticillium*, etc. (Nosanchuk et al., 2015). Since fungi play a key role in melanin degradation in nature (Nadhilah et al., 2023), they were believed to be a great potential source of cosmetic skin-whiteners. At present, several fungal metabolites have been proven to reduce melanin production by inhibiting tyrosinase. As such, *Aspergillus flavus* derived kojic acid (Ola et al., 2019), lactic acids, and glycolic acids from *Rhizopus* spp. (Zhang et al., 2007), myrothenones from *Myrothecium* sp. (Li et al., 2005), and sesquiterpenes isolated from *Pestalotiopsis* sp. (Wu et al., 2013) could be eligible for skin-whitener production. Additionally, increasing concerns regarding antibiotic resistance and the need to discover fresh active compounds against acne causing bacteria have made microfungi a source for mining new ingredients in skin-care formulations. In 2014, two fungal pyridones from *Trichoderma* sp. were identified with antibiotic activity against skin disorder inducing bacterium *Staphylococcus epidermidis*, with IC<sub>50</sub> values ranging from 4 to 24 µM (Wu et al., 2014). Concurrently, the properties of compound C from endophytic fungus *Talaromyces wortmannii* in *in vitro* anti-inflammation and the inhibition of *Propionibacterium acnes* are promising for new added active agents in cosmeceuticals against dermatological acne vulgaris (Pretsch et al., 2014). Although instances of adverse reaction, irritation, and skin allergies should be carefully considered, the cosmeceutical benefits of microfungal metabolites to the skin are obviously significant, making their application in skin care become an upcoming research trend.

Our study aims to characterize and examine cosmeceutical properties, i.e., the inhibitory effects of isolated fungal components on tyrosinase activity, lipase activity, and acne-causing bacteria, as well as to determine their *in vitro* wound-healing effects on fibroblasts.

## Materials and methods

### Taxonomic study

Marine and mangrove derived microbial strains CL6 and S3-Rt-N3 were isolated from thallus of *Padina australis* (Sampling site: N 12°13.848', E 109°14.505') and rhizosphere of *Sonneratia caseolaris* (Sampling site: N 20°12.226', E 106°33.009'), respectively. These were determined to be halotolerant with up to 5% NaCl (data not shown) and are deposited in the Institute of Natural Products Chemistry, Vietnam Academy of Science and Technology – either in forms of pure culture or cryopreserved vials.

Genomic DNA extraction was performed following the modified method of benzyl chloride (Zhu et al., 1993). Polymerase chain reaction (PCR) for amplification of internal transcribed spacer (ITS) region was carried out using universal fungal primers ITS1 (5'-TCCGTAGGTGAACCTGCGT-3') and ITS4 (5'-TCCTCCGCTTGATATGC-3') (White et al., 1990). The amplified PCR product was sequenced by 1st BASE DNA Sequencing Services (Malaysia).

These fungi were characterized by both an analysis of the obtained sequence by BLAST search in NCBI GenBank and morphological study (Visagie et al., 2014; Yilmaz et al., 2014).

### General procedure

Mass spectra were measured on a Thermo LCQ Fleet spectrometer (Thermo, USA). Nuclear magnetic resonance (NMR) spectra (<sup>1</sup>H-NMR, <sup>13</sup>C-NMR, DEPT, HSQC, HMBC, COSY and NOESY) data were measured on a Bruker Ascend 600 NMR spectrometer (Bruker, USA) to elucidate the structures of purified compounds. <sup>1</sup>H- and <sup>13</sup>C-NMR spectra were recorded at 600 MHz and 150 MHz, respectively, with tetramethylsilane (TMS) as an internal standard. Chemical shifts were expressed in δ (ppm) and coupling constants (J) in Hz. Column chromatography (CC) was prepared with silica gel 60 (70–230 mesh, Merck, Germany). High performance liquid chromatography (HPLC) separation was performed on Agilent 1200 Preparative HPLC System (Agilent Technologies, USA).

### Fermentation and crude extraction

Halotolerant fungal strains (*Penicillium* sp. CL6 and *Talaromyces* sp. S3-Rt-N3) were grown on potato dextrose agar (HiMedia, India) supplemented with 3% sodium chloride (pH 6.8) (potato dextrose-sea water agar) (30 °C, 14 days) and then transferred to Erlenmeyer flasks containing liquid medium of potato dextrose-sea water (pH 6.8) for inoculation. After 15 days, the broth (120 l each strain) was separated from mycelia by filtration (pore size 38 µm) and partitioned in triplicate with an equal volume of ethyl acetate (Xilong Scientific, China), followed by *in vacuo* evaporation (45 °C, 40 rpm) to yield concentrated crude extracts (10.3–12.7 g).

### Isolation and structure elucidation of chemical compounds

The EtOAc extracts of CL6 (12.7 g) and of S3-Rt-N3 (14.2 g) were separately subjected to reversed phase (RP) C<sub>18</sub> column chromatography (CC), using a gradient solution of 30, 70, and 100% MeOH in H<sub>2</sub>O to give rise to three fractions of CL6 (C6.1–C6.3) and three fractions of S3-Rt-N3 (S3.1–S3.3), respectively.

Fraction C6.3 was introduced to silica gel CC, using *n*-hexane-acetone (gradient 40:1→0:1, v/v) as eluent to yield 10 subfractions (C6.3.1–C6.3.10). Compound (1) (6.75 mg) was isolated by recrystallization technique for the removal of impurities and yielding a non-crystalline solid in a powdered form. C6.2 was separated by silica gel CC, eluting with CH<sub>2</sub>Cl<sub>2</sub>-MeOH (20:1, v/v) to provide C6.2.1. From the subfraction C6.2.1, compound (2) (3.0 mg) was isolated by purification through preparative HPLC, using acetonitrile in H<sub>2</sub>O (7:93, v/v) as a mobile phase.

From the fraction S3.3, 10 subfractions (S3.3.1–S3.3.10) were provided by silica gel CC with *n*-hexane-acetone (gradient 40:1→0:1, v/v) as eluent. Subfraction S3.3.10 was separated by silica gel CC, eluting with *n*-hexane-ethyl acetate (1.5:1, v/v) to provide S3.3.11. From the subfraction S3.3.11, compound (3) (5.4 mg) was obtained by silica gel CC with *n*-hexane-ethyl

acetate (1:3, v/v) as eluent. Compound (4) was isolated from subfraction S3.3.8 by silica gel CC, eluting with *n*-hexane-ethyl acetate (2:5:1, v/v) in combination with purification by recrystallization.

**(1):** White amorphous powder; ESI-MS (positive mode)  $m/z$  431  $[M+H]^+$ ;  $^1H$  NMR (600 MHz, DMSO-*d*<sub>6</sub>):  $\delta_H$  1.30 (2H, m, H-1), 1.23 (1H, m, H-2a), 1.60 (1H, m, H-2b), 3.77 (1H, m, H-3), 1.88 (1H, m, H-4a), 1.50 (1H, m, H-4b), 3.38 (1H, d,  $J$  = 5.4 Hz, H-6), 5.08 (1H, d,  $J$  = 4.8 Hz, H-7), 1.96 (1H, m, H-9), 1.40 (2H, m, H-11), 1.27 (1H, m, H-12a), 1.95 (1H, m, H-12b), 1.80 (1H, m, H-14), 1.37 (1H, m, H-15a), 1.48 (1H, m, H-15b), 1.25 (1H, m, H-16a), 1.66 (1H, m, H-16b), 1.25 (1H, m, H-17), 0.54 (3H, s, H-18), 0.91 (3H, s, H-19), 2.01 (H, dd,  $J$  = 15.4, 6.6 Hz, H-20), 0.99 (3H, d,  $J$  = 6.6 Hz, H-21), 5.17 (H, dd,  $J$  = 15.0, 7.2 Hz, H-22), 5.24 (H, dd,  $J$  = 15.0, 7.2 Hz, H-23), 1.86 (1H, m, H-24), 1.46 (1H, m, H-25), 0.81 (3H, d,  $J$  = 7.2 Hz, H-26), 0.80 (3H, d,  $J$  = 7.2 Hz, H-27), 0.89 (3H, d,  $J$  = 7.2 Hz, H-28).  $^{13}C$  NMR (150 MHz, DMSO-*d*<sub>6</sub>):  $\delta_C$  32.4 (C-1), 31.1 (C-2), 65.9 (C-3), 39.9 (C-4), 74.4 (C-5), 72.1 (C-6), 119.4 (C-7), 139.6 (C-8), 42.2 (C-9), 36.6 (C-10), 21.3 (C-11), 38.9 (C-12), 42.9 (C-13), 54.1 (C-14), 22.5 (C-15), 27.7 (C-16), 55.3 (C-17), 12 (C-18), 17.6 (C-19), 40.2 (C-20), 20.9 (C-21), 135.3 (C-22), 131.3 (C-23), 42 (C-24), 32.4 (C-25), 19.4 (C-26), 19.7 (C-27), 17.2 (C-28).

**(2):** White amorphous powder; ESI-MS (positive mode)  $m/z$  235  $[M+H]^+$ ;  $^1H$  NMR (500 MHz, CD<sub>3</sub>OD):  $\delta_H$  6.08 (1H, s, H-3), 6.65 (1H, d,  $J$  = 2.4 Hz, H-6), 6.68 (1H, d,  $J$  = 2.4 Hz, H-8), 1.29 (3H, d,  $J$  = 6.0 Hz, H-3'), 2.74 (3H, s, 5-CH<sub>3</sub>).  $^{13}C$  NMR (125 MHz, CD<sub>3</sub>OD):  $\delta_C$  167.1 (C-2), 112.5 (C-3), 182.0 (C-4), 143.8 (C-5), 118.2 (C-6), 163.2 (C-7), 101.9 (C-8), 161.7 (C-9), 116.0 (C-9), 44.4 (C-1'), 66.6 (C-2'), 23.9 (C-3'), 23.2 (5-CH<sub>3</sub>).

**(3):** White amorphous powder; ESI-MS (positive mode)  $m/z$  445  $[M+H]^+$ ;  $^1H$  NMR (500 MHz, acetone-*d*<sub>6</sub>):  $\delta_H$  0.67 (3H, s, H-18), 0.85 (3H, s, H-19), 1.05 (3H, d,  $J$  = 5.5 Hz, H-21), 0.99 (3H, d,  $J$  = 5.5 Hz, H-26), 0.84 (3H, d,  $J$  = 5.5 Hz, H-27), 0.95 (3H, d,  $J$  = 6.0 Hz, H-28), 5.58 (1H, s, H-7), 5.25 (1H, dd,  $J$  = 6.5, 13.0 Hz, H-22), 5.30 (1H, dd,  $J$  = 6.5, 13.0 Hz, H-23).  $^{13}C$  NMR (125 MHz, acetone-*d*<sub>6</sub>): 26.3 (C-1), 30.1 (C-2), 67.0 (C-3), 37.6 (C-4), 79.9 (C-5), 197.9 (C-6), 120.5 (C-7), 163.4 (C-8), 75.4 (C-9), 42.8 (C-10), 30.5 (C-11), 35.7 (C-12), 45.7 (C-13), 52.2 (C-14), 23.0 (C-15), 28.6 (C-16), 56.8 (C-17), 12.4 (C-18), 19.5 (C-19), 41.1 (C-20), 21.4 (C-21), 136.3 (C-22), 133.0 (C-23), 43.7 (C-24), 33.8 (C-25), 20.5 (C-26), 20.3 (C-27), 18.05 (C-28).

**(4):** White amorphous powder. ESI-MS (positive mode)  $m/z$  427  $[M+H]^+$ ;  $^1H$  NMR (600 MHz, CDCl<sub>3</sub>):  $\delta_H$  0.81 (3H, s, CH<sub>3</sub>-18), 0.82 (3H, d,  $J$  = 6.6 Hz, CH<sub>3</sub>-26), 0.83 (3H, d,  $J$  = 6.6 Hz, CH<sub>3</sub>-27), 0.88 (3H, s, CH<sub>3</sub>-19), 0.91 (3H, d,  $J$  = 6.5 Hz, CH<sub>3</sub>-28), 1.00 (3H, d,  $J$  = 6.6 Hz, CH<sub>3</sub>-21), 3.97 (1H, m, H-3), 5.15 (1H, dd,  $J$  = 7.5, 15.0 Hz, H-22), 5.21 (1H, dd,  $J$  = 7.5, 15.0 Hz, H-23), 6.24 (1H, d,  $J$  = 8.5 Hz, H-6), 6.50 (1H, d,  $J$  = 8.5 Hz, H-7).  $^{13}C$  NMR (150 MHz, CDCl<sub>3</sub>):  $\delta_C$  34.7 (C-1), 30.1 (C-2), 66.5 (C-3), 36.9 (C-4), 82.1 (C-5), 135.4 (C-6), 130.7 (C-7), 79.4 (C-8), 51.1 (C-9), 37.0 (C-10), 20.6 (C-11), 39.4 (C-12), 44.6 (C-13), 56.2 (C-14), 23.4 (C-15), 28.6 (C-16), 56.2 (C-17), 12.9 (C-18), 18.2 (C-19), 39.7 (C-20), 20.8 (C-21), 135.2 (C-22), 132.3 (C-23), 42.7 (C-24), 33.1 (C-25), 19.6 (C-26), 19.9 (C-27), 17.6 (C-28).

### Cell culture and test bacteria

NIH-3T3 embryonic murine fibroblasts originated from the American Type Culture Collection (CRL-1658, ATCC, USA) and was cultured in Dulbecco's Modified Eagle Medium (DMEM) supplemented with 10% fetal bovine serum (FBS), 1% streptomycin (Corning, USA), incubated at 37 °C, 5% CO<sub>2</sub> with medium change every two days.

Test bacterium *Propionibacterium acnes* ATCC 11827 was inoculated in Brain Heart Infusion medium (BHI, HiMedia, India) at 37 °C, 5% CO<sub>2</sub>.

### Antibacterial assay

The antimicrobial activity of isolated compounds was determined on 96-well plates, according to the previously described broth dilution method (Vanden Berghe and Vlietinck, 1991). The bacterial suspension was briefly adjusted to a concentration of 10<sup>6</sup>–10<sup>7</sup> CFU/ml with BHI broth, and subsequently added to serial diluted solutions of test sample. The microplates were then incubated for 48 h at 37 °C for observation of microbial growth and determination of the minimum inhibitory concentration (MIC). Streptomycin (Sigma-Aldrich, Germany) was employed as the positive control.

### Tyrosinase inhibitory assays

Tyrosinase inhibitory activities of isolated compounds were examined against mushroom tyrosinase (EC 1.14.18.1, Sigma-Aldrich, Germany) by dopachrome method using both substrates L-tyrosine and L-3,4-dihydroxyphenylalanine (L-DOPA) (Merck, Germany) on 96-well plates.

Using L-tyrosinase substrate, the inhibitory assay was carried out following Khatib et al. (2005) with minor modifications. Accordingly, test compounds were pre-incubated (37 °C, 5 min) with 100 U/ml tyrosinase in potassium phosphate buffer (50 mM, pH = 6.5). Thereafter 100 µl of substrate solution containing L-tyrosine 2 mM (Sigma-Aldrich, Germany) was added to the mixture and incubated (37 °C, 60 min) for reaction.

The tyrosinase inhibitory assay employing L-DOPA substrate was conducted as described by Lim et al. (1999) with modifications. Mushroom tyrosinase and dissolved test compound were briefly pre-incubated in potassium phosphate buffer (50 mM, pH = 6.5) at 37 °C. After 5 min, 50 µl of L-DOPA (3 mM) was added and further incubated (37 °C, 30 min).

The formation of product dopachrome was measured spectrophotometrically (absorption at 475 nm) by microplate reader (Tecan F150, Switzerland). Kojic acid (Sigma-Aldrich, Germany) was used as positive reference. The tyrosinase inhibition rates by test compounds were expressed as percentages (TI, %) against control (1% DMSO instead of test compound in potassium phosphate buffer) resulting from the following formula:

$$TI (\%) = \{1 - [(A_S - A_B)/(A_C - A_N)]\} * 100\%$$

where A<sub>S</sub> and A<sub>B</sub> are absorbances at 475 nm of test compound in the presence and absence of enzyme, respectively; A<sub>C</sub> and A<sub>N</sub> are absorbances of control in the presence and absence of enzyme, respectively.

### Cell proliferation assay

NIH-3T3 fibroblasts were seeded (2.5 × 10<sup>4</sup> cells/ml) in DMEM medium supplemented with 10% FBS in each well of a 96-well plate and incubated (37 °C, 5% CO<sub>2</sub>) until 70–80% confluent.



cy. Cells were then exposed to medium change with DMEM medium supplemented with 1% FBS to improve uniformity and treated with either 0.5% DMSO (negative control) or test samples for 48 h (37 °C, 5% CO<sub>2</sub>). The viable proliferated cells after treatments were evaluated by (3-(4,5-dimethylthiazol-2-yl)-2,5-diphenyltetrazolium bromide (MTT) colorimetric method (Berridge et al., 2005). Accordingly, cell culture medium was replaced by fresh medium containing 0.5 mg/ml MTT and incubated (4 h, 37 °C, 5% CO<sub>2</sub>). After discarding the supernatant, remaining formazan crystals were solubilized in 100% DMSO for absorbance measurement at 570 nm (Tecan F150, Switzerland).

### Scratch assay

Wound healing activity of test compounds were investigated *in vitro* by scratch assay (Liang et al., 2007) on 24-well plates using SPLScar™ Scratcher (SPL Life Science, Korea). For assessment, NIH-3T3 cells were grown at a density of  $2 \times 10^4$  cells/ml and incubated (24 h, 37 °C, 5% CO<sub>2</sub>) until formation of cell monolayer. Subsequently, scratcher tips (1 mm width) were applied to produce uniform wound areas in each well of the plates. After being rinsed with potassium phosphate buffer, fresh medium (DMEM, 1% FBS) was introduced, and cell culture was incubated with either test samples or 0.5% DMSO (37 °C, 5% CO<sub>2</sub>). Wound healing areas were imaged at 0, 48, and 72 h (Olympus, Japan), and analyzed using ImageJ software (Schneider et al., 2012). Relative wound closure rates were estimated as percentages of wound closure areas in initial wound areas as mentioned (Zhang et al., 2018).

### Statistical analysis

Experiments were carried out in triplicate and all data are expressed as mean  $\pm$  SD (Standard Deviation). Comparison of

variances within groups was conducted using one-way analysis of variance (ANOVA), while Student's *t*-test was employed for paired comparison between groups. *P* values less than 0.05 were considered statistically significant. The half maximal inhibitory concentration (IC<sub>50</sub>) was estimated by nonlinear regression analysis using the computer software TableCurve 2D version 5.1 (Systat Software, USA).

## Results and discussion

### Fungal taxonomy

On Czapek Dox Agar medium (CDA, HiMedia, India), strain CL6 appeared as fast-growing colonies, reaching an average diameter of 4 cm after 10 days of incubation at 25 °C. The colonies' surface was fuzzy, beige in color at the centre, and whitish in the margin (Fig. 2A). Micromorphologically, conidiophores (50.0–200.0  $\times$  3.0–4.0  $\mu$ m) with branched metulae and ellipsoidal conidia (2.5–4.5  $\times$  2.0–3.0  $\mu$ m), spherical mature cleistothecium (150–250  $\mu$ m in diameter) containing 8 asci (7.0–9.0  $\mu$ m in diameter) and spherical to ellipsoidal ascospores (3.5–5.0  $\times$  2.5–3.0  $\mu$ m) were observed (Fig. 1B, C).

Macromorphologically, colonies of strain S3-Rt-N3 on CDA plates were fast-growing, bright yellow, slightly raised at the centre. They were observed to have low, entire and white margins after 7 days of incubation at 25 °C. After 10 days, the production of soluble yellow to orange yellow pigments was noted. Under the microscope, characteristically symmetrically biverticillate conidiophores, branched metulae, and ellipsoidal conidia (2–4  $\times$  1.5–3.0  $\mu$ m) were observed. Stipes were smooth walled (10–100  $\times$  2–2.5  $\mu$ m) (Fig. 1D–F).

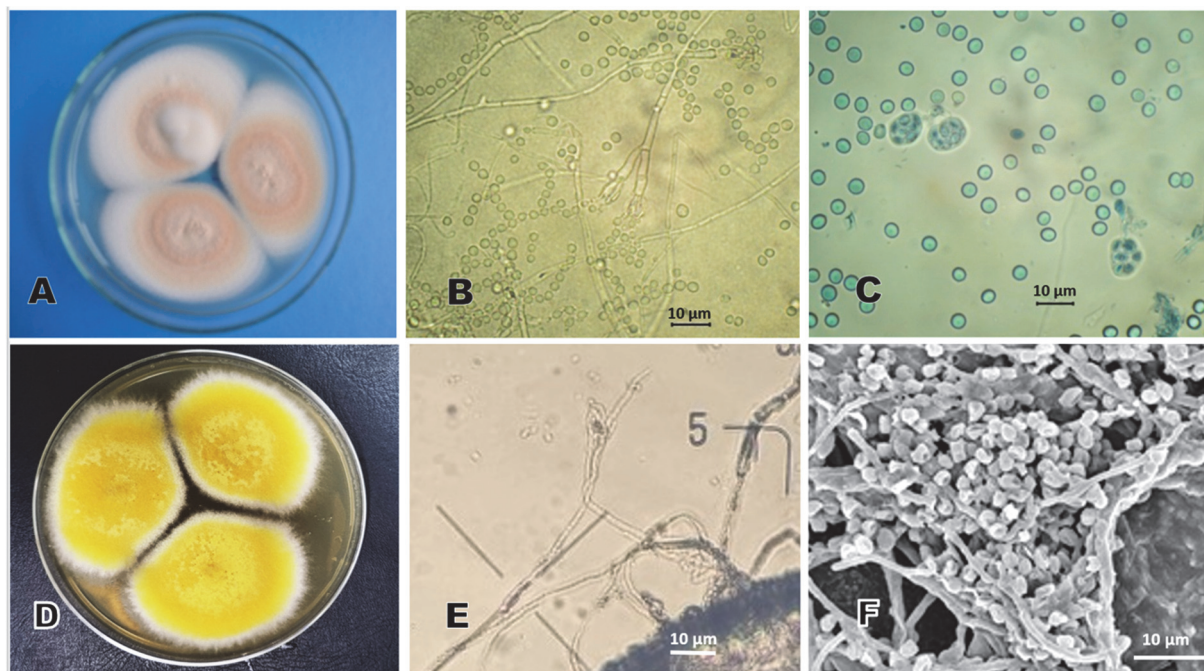


**Fig. 1.** Morphological characteristics of fungal strains CL6 and S3-Rt-N3. (A) CL6's colonial morphology on CDA medium (25 °C, 10 days); (B) CL6's conidiophores and conidia; (C) CL6's asci and ascospores ( $\times 1000$ ); (D) S3-Rt-N3's colonial morphology on CDA medium (25 °C, 10 days); (E) S3-Rt-N3's conidiophores and conidia; (F) S3-Rt-N3's ascospores ( $\times 1000$ ).

Based on the sequence of amplified 510–547 bp long ITS regions from fungal strains CL6 (Genbank: OR298248.1) and S3-Rt-N3 (Genbank: SUB14654410), the taxonomical relationship of these to identified *Penicillium* and *Talaromyces* species resulting from BLAST search in GenBank was revealed (Fig. 2).

The integration of the above characteristics suggested the taxonomy of CL6 as a fungal strain of *P. brefeldianum* DODGE

(Visagie et al., 2014), and strain S3-Rt-N3 as a fungus of *Talaromyces* sect. *Talaromyces* (Yilmaz et al., 2014). The isolation and structural elucidation of four compounds from EtOAc extracts of *P. brefeldianum* strain CL6 and *Talaromyces* sp. and S3-Rt-N3, as well as the evaluation of their *in vitro* cosmeceutical activities are mentioned in the next sections of the manuscript.

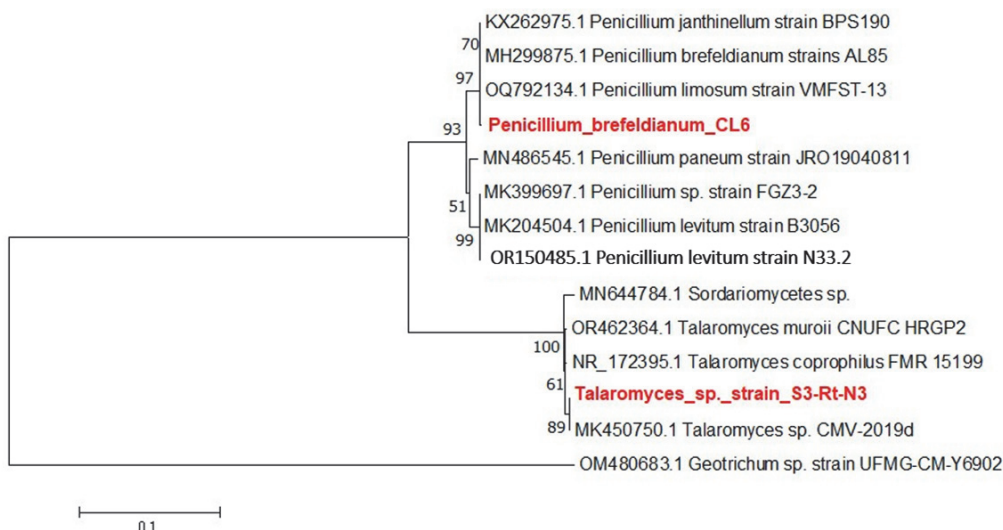


**Fig. 2.** Phylogeny of the ITS regions of strains CL6, S3-Rt-N3, and related species (Neighbor joining algorithm, bootstrap 1000). *Geotrichum* sp. strain UFMG-CM-Y6902 (Genbank: OM480683.1) was selected as an out-group.

### Structures of the fungal metabolites

**Compound (1).** The data obtained from  $^{13}\text{C}$ -NMR and DEPT spectra revealed the signal of 28 carbons, including 6 methyl groups, 7 methylenes, 11 methines, and 4 quaternary carbons. In combination with the ESI-MS at  $m/z$  431, the molecular formula was deduced as  $\text{C}_{28}\text{H}_{46}\text{O}_3$ . From the  $^1\text{H}$ -NMR spectral data, the existence of 6 methyl groups [ $\delta_{\text{H}}$  0.54 (3H, s, H-18), 0.90 (3H, s, H-19), 0.99 (3H, d,  $J = 5.5$  Hz, H-21), 0.80 (3H, d,  $J = 6.0$  Hz, H-26), 0.81 (3H, d,  $J = 6.0$  Hz, H-27) and 0.89 (3H, d,  $J = 6.0$  Hz, H-28)] and 3 olefinic protons [ $\delta_{\text{H}}$  5.08 (1H, d,  $J = 2.0$ , H-7), 5.17 (1H, dd,  $J = 6.0$ , 12.5 Hz, H-22), 5.23 (1H, dd,  $J = 6.0$ , 12.5 Hz, H-23)] was exhibited. HMBC spectral data suggested the correlations of H-18 ( $\delta_{\text{H}}$  0.54 Hz) ( $\delta_{\text{C}}$  5.34) to C-12 ( $\delta_{\text{C}}$  39.0), C-13 ( $\delta_{\text{C}}$  42.9) and C-14 ( $\delta_{\text{C}}$  54.1), H-19 to C-1 ( $\delta_{\text{C}}$  32.4), C-5 ( $\delta_{\text{C}}$  74.4) and C-10 ( $\delta_{\text{C}}$  36.6), from H-21 ( $\delta_{\text{C}}$  0.99 Hz) to C-20 ( $\delta_{\text{C}}$  39.9)/C-22 ( $\delta_{\text{C}}$  131.3)/C-17 ( $\delta_{\text{C}}$  55.2); from H-28 to C-23/C-24/C-25; from H-26/H-27 to C-26/27/C-25, indicating positions of methyl groups at C-10, C-13, C-20, C-24 and C-25. Besides, positions of methylene and methine groups at  $\delta_{\text{C}}$  32.4 (C-1), 31.1 (C-2), 40.1 (C-4), 21.2 (C-11), 39.0 (C-12), 22.5 (C-15), 27.6 (C-16), 65.9 (C-3), 72.0 (C-6), 119.4 (C-7), 42.2 (9), 54.1 (C-14), 55.2 (C-17), 39.9 (C-20), 131.3 (C-22), 135.3 (C-23) and 32.4 (C-25) were determined.

**Compound (2).** The  $^{13}\text{C}$ -NMR and HSQC spectra of (2) revealed the presence of 13 carbons, including two methyl, 4 methylenes, one methine group, and 6 quaternary carbons. The molecular formula  $\text{C}_{13}\text{H}_{14}\text{O}_4$  ( $M = 234$ ) was deduced from these analyzed spectra and the ESI-MS ion at  $m/z$  235  $[\text{M}+\text{H}]^+$ . The  $^1\text{H}$ -NMR spectrum showed olefinic proton signals at  $\delta_{\text{H}}$  6.08 (1H, s, H-3), 6.65 (1H, d,  $J = 2.4$  Hz, H-6) and 6.68 (1H, d,  $J = 2.4$  Hz, H-8), two methyl proton signals at  $\delta_{\text{H}}$  1.29 (3H, d,

$J = 6.0$  Hz, H-3') and 2.74 (3H, s, 5- $\text{CH}_3$ ), and one oxymethine group at  $\delta_{\text{H}}$  4.20 (1H, m, H-2'). In the HMBC spectrum, correlations from H-3' ( $\delta_{\text{H}}$  1.29) to C-1' ( $\delta_{\text{C}}$  44.2)/C-2' ( $\delta_{\text{C}}$  66.3) and from  $\text{CH}_3$  ( $\delta_{\text{H}}$  2.74) to C-5 ( $\delta_{\text{C}}$  143.6) were displayed, indicating the presence of two methyl groups at C-2' and C-5. Further, HMBC correlations from H-3 ( $\delta_{\text{H}}$  6.08) to C-2/C-6/C-10 and from H-6/H-8 to C-7/C-8/C-6 were also revealed.

By comparing these fungal constituents' spectral data with those previously published in the literature (Gao et al., 2013; Palama et al., 2009; Sharma et al., 2011), compounds (1) and (2) were determined as 3 $\beta$ ,5 $\alpha$ ,6 $\beta$ -trihydroxy-ergosta-7,22-diene (cervisterol) and 7-hydroxy-2-(2'-hydroxypropyl)-5-methyl-4H-chromen-4-one (aloesol), respectively (Fig. 3).

**Compound (3).** The molecular formula was established as  $\text{C}_{28}\text{H}_{44}\text{O}_4$  ( $M = 444$ ) by a protonated molecular ion  $[\text{M}+\text{H}]^+$  at  $m/z$  445 in the ESI-MS in combination with an analysis of the  $^1\text{H}$  and  $^{13}\text{C}$ -NMR spectra. The  $^1\text{H}$ -NMR spectrum exhibited signals of 6 methyl groups at  $\delta_{\text{H}}$  0.67 (3H, s, H-18), 0.85 (3H, s, H-19), 1.05 (3H, d,  $J = 5.5$  Hz, H-21), 0.99 (3H, d,  $J = 5.5$  Hz, H-26), 0.84 (3H, d,  $J = 5.5$  Hz, H-27) and 0.95 (3H, d,  $J = 6.0$  Hz, H-28). The  $^1\text{H}$ -NMR additionally showed signals of three olefinic protons at  $\delta_{\text{H}}$  5.58 (1H, s, H-7), 5.25 (1H, dd,  $J = 6.5$ , 13.0 Hz, H-22), 5.30 (1H, dd,  $J = 6.5$ , 13.0 Hz, H-23). The  $^{13}\text{C}$ -NMR and the HSQC spectra contained signals of 28 carbons, including 6 primary, 7 secondary, 9 tertiary, and 6 quaternary carbons. In general, the spectral data of compound (3) exhibited similarities to those of (1), except for the existence of a carbonyl group ( $\text{C} = \text{O}$ ) at  $\delta_{\text{C}}$  197.9 instead of hydroxyl group at C-6 as deduced in the molecular formula of (1). Comparison of the  $^1\text{H}$  and  $^{13}\text{C}$  NMR data of (3) with those of the reported literature (Xiong et al., 2009) revealed a good match,

suggesting the similarity of both structures. Compound (3) was determined to be  $3\beta,5\alpha,9\alpha$ -trihydroxyergosta-7,22-diene-6-one (Fig. 3).

**Compound (4).** From the ESI-MS  $[M+H]^+$  at  $m/z$  429 and the  $^{13}\text{C}$ -NMR spectrum revealing signals of 28 carbons, including 6 methyl [at  $\delta_{\text{C}}$  12.9 (C-18), 18.2 (C-19), 20.8 (C-21), 19.6 (C-26), 19.9 (C-27), and 17.6 (C-28)], 7  $\text{sp}^3$  methylene and 4 quaternary carbons, and two disubstituted olefins at  $\delta_{\text{C}}$  135.4 (C-6), 130.7 (C-7), 135.2 (C-22), 132.3 (C-23), the molecular formula of (4) was deduced as  $\text{C}_{28}\text{H}_{44}\text{O}_3$  ( $M = 428$ ). The chemical shifts of C-3 ( $\delta_{\text{C}}$  66.5), C-5 ( $\delta_{\text{C}}$  82.1), and C-8 ( $\delta_{\text{C}}$  79.4), suggested its linkage to oxygen. Two oxygenated quaternary carbons of C-5 ( $\delta_{\text{C}}$  82.1), and C-8 ( $\delta_{\text{C}}$  79.4) suggested the presence of a peroxide structure. The  $^1\text{H}$ -NMR spectrum revealed the existence of 6 methyl signals including 2 singlets at  $\delta_{\text{H}}$  0.81 (3H, s, H-18), and 0.88 (3H, s, H-19) and 4 doublets at  $\delta_{\text{H}}$  0.82 (3H, d,  $J = 6.6$  Hz, H-26), 0.83 (3H, d,  $J = 6.6$  Hz, H-27), 0.91 (3H, d,  $J = 6.5$  Hz, H-28), 1.00 (3H, d,  $J = 6.6$  Hz, H-21), and

one oxymethine proton at  $\delta_{\text{H}}$  3.97 (1H, m, H-3). The signals at  $\delta_{\text{H}}$  6.24 (1H, d,  $J = 8.5$  Hz, H-6), 6.50 (1H, d,  $J = 8.5$  Hz, H-7) in the  $^1\text{H}$ -NMR spectrum revealed the presence of a disubstituted double bond which correlated with carbon signals of  $\delta$  135.4 (C-6) and 130.7 (C-7) in HMBC spectrum. The 2D-NMR experiments confirmed that compound (4) is a steroid, containing a peroxy function at C-5/C-8 and two double bonds at C-6/C-7 and C-22/C-23. The HMBC correlations of Me-18 with C-12/C-13/C-14/C-17 demonstrated the position of this methyl at C-13. The remaining five methyl groups could be positioned at C-10, C-20, C-24, and C-25 on the basis of the HMBC correlations between Me-19 and C-1/C-5/C-9/C-10; between Me-21 and C17/C-20/C-22; between Me-28 and C-23/C-24/C-25; and between Me-26 and Me-27 and C-25/C-24, and the correlation of the respective methyl carbons to each other. Other 2D-NMR spectra supported the structure of (4) as ergosterol peroxide. The  $^1\text{H}$ - and  $^{13}\text{C}$ -NMR data were in good agreement with the literature values (Krzyczkowski et al., 2009), supporting the notion of compound (4) as ergosterol peroxide (Fig. 3).

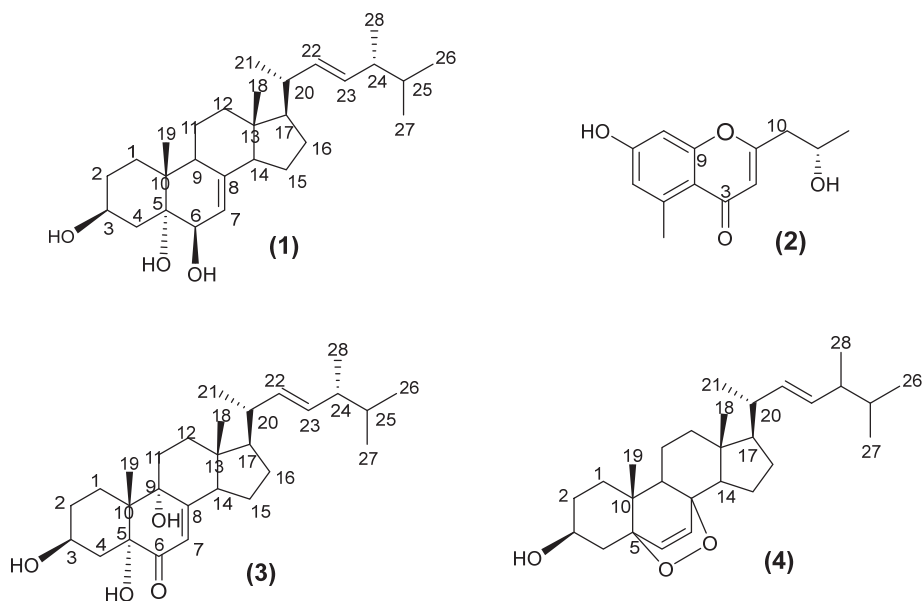


**Fig. 3.** Structures of isolated compounds from fungal strains CL6 and S3-Rt-N3. (1) cerevisterol; (2) aloesol; (3)  $3\beta,5\alpha,9\alpha$ -trihydroxyergosta-7,22-diene-6-one; (4) ergosterol peroxide

Aloesol (2), along with ergosterol derivatives, including cerevisterol (1),  $3\beta,5\alpha,9\alpha$ -trihydroxyergosta-7,22-diene-6-one (3), and ergosterol peroxide (4), are widely-distributed secondary metabolites in the plant and fungi kingdoms and have been reported with diverse biological activities (Majhi and Das, 2021; Sharma et al., 2011; Singh et al., 2021; Ye et al., 2021). However, the cosmeceutical properties of these compounds, especially those with fungal derivation, have not been investigated elsewhere. Furthermore, biological assessments of such metabolites could support data for better understandings concerning biochemical profile of halotolerant fungal symbionts.

### Antimicrobial activity

Skin diseases are typically due to successive exposure to damaging factors, particularly chemical agents and associated microbiota. As commonly known, microbes are disseminated on human skin depending on environmental and health conditions. Most of these are commensal and opportunistic, which can turn to pathogenic form when human immune system

is attenuated. In most circumstances, infectious bacteria are harmful, thus antimicrobial ingredients are the first choice for dermal therapeutic approach. The antibacterial assay for compounds (1) and (2) isolated from *P. brefeldianum* CL6 and (3) and (4) from *Talaromyces* sp. strain S3-Rt-N3 was carried out with test bacterium *P. acnes*. The results revealed the ability of cerevisterol (1) in inhibiting skin pathogen *P. acnes* with MIC = 200  $\mu\text{g}/\text{ml}$  (~464  $\mu\text{M}$  equivalent), while no inhibition was observed in the presence of (2), (3), and (4) (Table 1).

The antimicrobial capacity of fungal cerevisterol has been mentioned (Appiah et al., 2020), whereby the *Trametes gibbosa* and *T. elegans* derived compound exhibited inhibitory effect against test bacteria *Salmonella typhi*, *S. aureus*, and *Enterococcus faecalis* with MICs  $\leq 50$   $\mu\text{g}/\text{ml}$ . Our study showed an updated extent of antibacterial potency of the steroidal ingredient, with a lowered inhibition against human pathogens. The discovery contributed to highlight the potential of natural fungal compounds as anti-acne agents, encouraging further studies on topical products of fungal origin.



**Table 1. Antibacterial property against *P. acnes* of isolated compounds from *P. brefeldianum* CL6 and *Talaromyces* sp. S3-Rt-N**

Sample	Concentration (µg/ml)	<i>Propionibacterium acnes</i>	
		Visible growth**	MIC (µg/ml)
(+) control*	60	–	30
	200	–	200
Compound (1)	100	+	
	50	+	
Compound (2)	200	+	–
	100	+	
	50	+	
Compound (3)	200	+	–
	100	+	
	50	+	
Compound (4)	200	+	–
	100	+	
	50	+	

Note: \* (+) control: Streptomycin (Merck, Germany); \*\* Symbols: +/– indicates visible/no visible growth of the test bacterium.

### Tyrosinase inhibitory activity

Based on the characteristic of tyrosinase in catalyzing two distinct reactions, i.e., the hydroxylation of L-tyrosine to L-DOPA, and the oxidation of L-DOPA to o-dopachrome (Chang, 2009; Pisano et al., 2024), tyrosinase inhibitory effects of cerevisterol (1), aloesol (2), 3β,5α,9α-trihydroxyergosta-7,22-diene-6-one (3), and ergosterol peroxide (4) were assayed by using both substrates.

The results indicated inhibitory effects against tyrosinase of isolated compounds (1), (3), and (4) when employing L-tyrosine as the substrate, with 75.14 ± 4.22%, 60.50 ± 3.96%, and 82.70 ± 3.40 % inhibition at 250 µM, respectively (Table 2). With L-DOPA as the substrate, the activity was roughly reduced, whereby the most significant inhibitory rates peaked 53.50 ± 2.64% when incubating with 250 µM of compound (4).

In general, among the three isolated fungal compounds, ergosterol peroxide (4) was the only one to exhibit an inhibitory effect against the conversion of both L-tyrosine and L-DOPA to dopachrome.

As shown in Table 2, with L-tyrosine as a substrate, the IC<sub>50</sub> values of ergosterol peroxide (4), cerevisterol (1), and 3β,5α,9α-trihydroxyergosta-7,22-diene-6-one (3) were 46.93, 51.98, and 225.45 µM, respectively, compared to IC<sub>50</sub> = 12.54 µM of kojic acid, indicating these compounds were not as potent as kojic acid in inhibiting tyrosinase. It was noted that these three isolated compounds exhibited inhibitory effects against tyrosinase with the substrate L-tyrosine (IC<sub>50</sub> = 46.93–225.45 µM) but showed weakened impacts on the induction of activity by L-DOPA (IC<sub>50</sub> > 145 µM). A similar tendency was observed by aloesol (2), where a concentration-

**Table 2. Tyrosinase inhibitory effects of isolated compounds from *P. brefeldianum* CL6 and *Talaromyces* sp. S3-Rt-N3 in substrates L-tyrosine and L-DOPA**

Sample	Concentration (µM)	L-tyrosine substrate		L-DOPA substrate	
		Inhibition rate (%)	IC <sub>50</sub> (µM)	Inhibition rate (%)	IC <sub>50</sub> (µM)
Kojic acid	25	80.92 ± 3.76	12.54	44.12 ± 5.06	25.77
	250	75.14 ± 4.22		19.82 ± 4.15	
Compound (1)	50	42.63 ± 3.82	51.98	8.61 ± 2.93	>250
	10	15.10 ± 2.97		2.42 ± 2.75	
Compound (2)	250	23.41 ± 5.11		0	
	50	12.81 ± 3.09	>250	0	–
	10	5.37 ± 2.35		0	
Compound (3)	250	60.50 ± 3.96		6.13 ± 3.08	
	50	29.39 ± 3.34	225.45	0	–
	10	10.66 ± 4.51		0	
Compound (4)	250	82.70 ± 3.40		53.50 ± 2.64	
	50	57.17 ± 4.22	46.93	30.26 ± 3.59	147.38
	10	25.95 ± 3.05		11.86 ± 3.66	

dependent inhibition against the enzyme in the L-tyrosine substrate but negligible effect in the substrate L-DOPA was recorded. Hypothetically, these fungal secondary metabolites might inhibit tyrosinase in an uncompetitive manner. Accordingly, they might bind to enzyme–substrate complex (L-tyrosine-Tyrosinase) instead of specific binding to the enzyme's active site. In other aspects, these compounds might selectively inhibit monophenolase activity of tyrosinase through competitive binding to the enzyme. Notwithstanding the differences between these hypotheses of inhibitory action mechanisms, our findings contributed to depict the diversity in biochemical modes of action of natural products.

As mentioned, several marine derived fungal metabolites were found as potent tyrosinase inhibitors, such as myrothenones from *Myrothecium* sp. ( $IC_{50} = 0.8 \mu M$ ) (Li et al., 2005), and two new sesquiterpenes isolated from *Pestalotiopsis* sp. strain Z233 with  $IC_{50}$  values of  $14.8 \mu M$  and  $22.3 \mu M$ , respectively (Wu et al., 2013). Along with these, our results ensure the continuation of search for fungal secondary metabolites for the prevention and treatment of hyperpigmentation. Besides, the potential for preparing new effective inhibitors from these isolated fungal materials by semisynthesis and biological modification is limitless. Regarding medical and health concerns, tyrosinase inhibitors have become a developing strategy in anti-Parkinson's disease (PD) compounds' discovery, owing to their possible role in mediating the occurrence of PD by inhibiting the generation of neuromelanin and the abnormality of redox-related protein level (Pisano et al., 2024; Qi et al., 2024; Wang et al., 2023). In particular, the side-reaction of L-DOPA to dopaquinone is known to be detrimental to the internal metabolic system and the availability of beneficial dopamine in the context of PD therapy (Qi et al., 2024). Herein, a microbe derived ergosterol peroxide was found as the enzyme's inhibitor in both substrates L-DOPA and L-tyrosine, thus it is significant for further consideration as a promising therapeutic medication – especially in the prevention of possible L-DOPA's damaging conversion products.

### Effects on fibroblast proliferation and migration

Skin wound repair is a multi-stage process in which cell proliferation and migration of fibroblasts are involved (Zhou et al., 2020). To investigate pharmaceutical aspects of isolated com-

pounds from *P. brefeldianum* CL6 and *Talaromyces* sp. strain S3-Rt-N3, their effects on murine fibroblast NIH-3T3's proliferation and migration were evaluated.

By means of MTT method, the effects of cerevisterol (1), aloesol (2),  $3\beta,5\alpha,9\alpha$ -trihydroxyergosta-7,22-diene-6-one (3), and ergosterol peroxide (4) on fibroblast cell viability and proliferation were investigated over a range of concentrations (2.5–20  $\mu g/ml$ ). The results depicted in Fig. 4 indicated that both compounds (1) and (2) were not only non-toxic to NIH-3T3 cells, but also promoted the cell proliferation at investigated concentrations, with (1) inducing a higher proliferation (up to  $112.07 \pm 0.32\%$  at 5  $\mu g/ml$ ) when compared to (2) (peaked  $108.01 \pm 0.45\%$  at 10  $\mu g/ml$ ). In a further perspective, these substances could be beneficial for wound healing and tissue repair, though it is recommended to be carefully considered, since the intensive exposure of the tissues to cell promoting agents may be associated with increased cancer risks. Accordingly, additional information on their cell division stimulating effect and genetic mutation is required. Generally, the increase of cell viability was observed when being treated with (1) and (2) at up to 10  $\mu g/ml$  before it slightly decreased at higher concentrations (Fig. 4). The incubation with compounds (3) and (4) from 2.5–20  $\mu g/ml$  however caused a lower cell viability of murine fibroblasts. At 20  $\mu g/ml$ , ergosterol peroxide (4) resulted in cytotoxicity of NIH-3T3 cells with cell survival rate at 0%, while the rate by (3) was  $76.35 \pm 2.01\%$  (Fig. 4). In essence, compound (4) was found cytotoxic at a concentration-dependent manner. Therefore, its wound-healing potential could be considerable in aspects of inflammatory responses, fibroblast migration, and re-epithelialization (Peña and Martin, 2024) once its non-toxic concentrations are determined. As a final point, fungal ergosterol peroxide was previously evidenced to cause apoptotic cell death without necrosis effect (Liu et al., 2024), thus its application in skincare is expectantly controllable and potentially advantageous in helping to prevent the skin from cancer by eliminating pre-malignant cells and harmful genetic changes.

Since mammalian fibroblasts have been known as a component of skin extracellular matrix, which is responsible for producing connective tissue and collagen (Myers et al., 2014), the induction for proliferating these cells may enhance re-epithelialization of the wound surface and regeneration of damaged

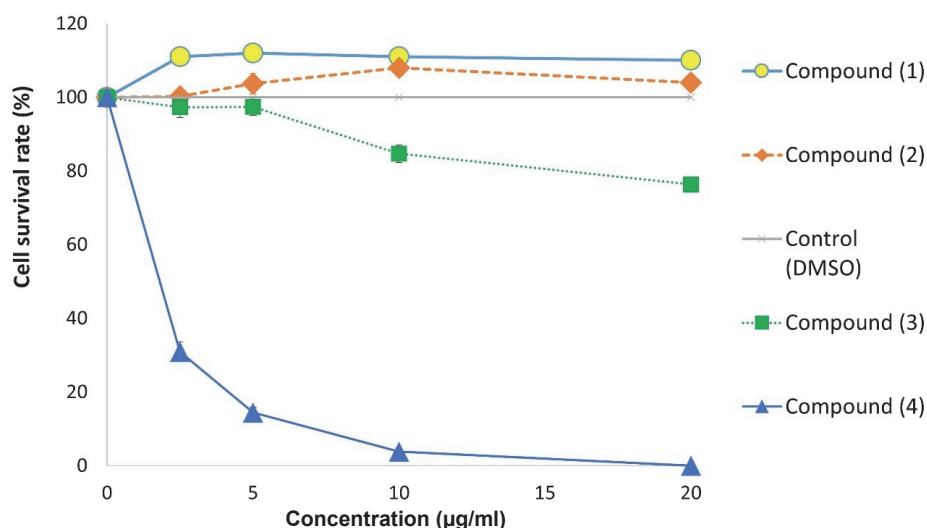


**Fig. 4.** NIH-3T3 cell viability after 48 hours of incubation with isolated compounds from *P. brefeldianum* strain CL6 and *Talaromyces* sp. strain S3-Rt-N3

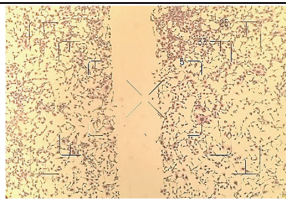
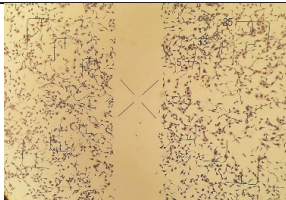
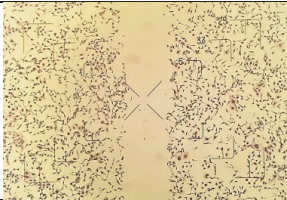
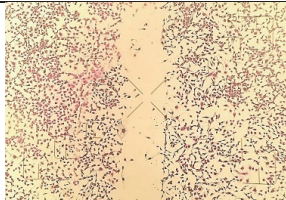
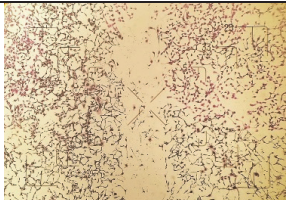
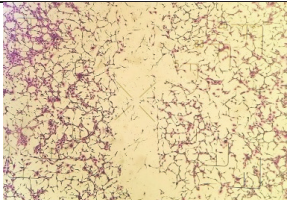
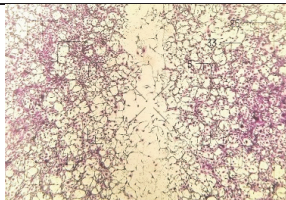
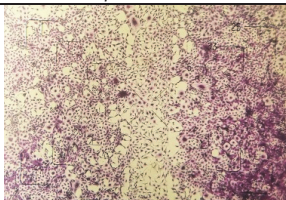
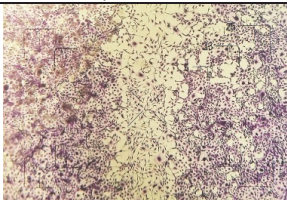


skin. As an ongoing effort to deepen the investigation of the wound healing properties of cerevisterol (1) and aloesol (2), their effects on *in vitro* migration of fibroblasts were assessed.

Table 3 illustrated the significant differences in the total and mitotic cell numbers after introducing *in vitro* two-dimensional wounds by scratching in a 48-h interval. As presented, at a test concentration of 20 µg/ml, both (1) and (2) enhanced the migration from the edge of the wound toward the empty

gap area (Table 3). At 48 h, the rate of wound closure for treatments with (1) and (2) was slightly increased ( $19.50 \pm 3.23$  and  $20.41 \pm 3.59\%$ ) compared to the control ( $12.37 \pm 2.15\%$ ). The relative rates of wound closure in the presence of cerevisterol (1) and aloesol (2) after 72 h were  $76.62 \pm 4.04$  and  $71.66 \pm 3.37\%$ , respectively, which were significantly higher ( $p < 0.05$ ) in comparison to vehicle ( $51.80 \pm 3.45\%$ ).

**Table 3. Effects of isolated fungal compounds on NIH-3T3 fibroblast cell migration\*, \*\***

Time point	Wound closure rates (%)		
	Control	Cerevisterol (1)	Aloesol (2)
Day 0			
	$0.03 \pm 0.01$	$0.01 \pm 0.01$	$0.02 \pm 0.01$
		$p > 0.05$	$p > 0.05$
Day 2 (48 h)			
	$12.37 \pm 2.15$	$19.50 \pm 3.23$	$20.41 \pm 3.59$
		$p < 0.05$	$p < 0.05$
Day 4 (72 h)			
	$51.80 \pm 3.45$	$76.62 \pm 4.04$	$71.66 \pm 3.37$
		$p < 0.05$	$p < 0.05$

Fibroblasts are known to play a crucial role in all phases of the wound healing process by producing a number of regulatory and cell signaling molecules (Cialdai et al., 2022). Thus, the effects of isolated fungal cerevisterol and aloesol to promote *in vitro* fibroblasts proliferation and migration are of great significance. The results of these assessments have revealed new candidates for successive *in vivo* studies and suggest the application potential of isolated fungal compounds for dermal cosmeceutical purposes, especially for repairing the skin from physical damage – such as injury and skin ageing.

## Conclusion

The emergence of microorganisms as a novel source of cosmetic ingredients has paved the way for sustainable development of the beauty industry. In this study, the bioassay guided approach has led to the finding of metabolites with cosmeceutical potentials from microfungi. As such, three compounds of er-

gosterol derivatives, i.e., cerevisterol,  $3\beta,5\alpha,9\alpha$ -trihydroxyergosta-7,22-diene-6-one, and ergosterol peroxide isolated from *P. brefeldianum* strain CL6 and *Talaromyces* sp. strain S3-Rt-N3, were found to demonstrate an inhibitory effect against tyrosinase *in vitro*. Of these, ergosterol peroxide exhibited the most potent enzyme inhibition in both substrates L-tyrosine and L-DOPA. Cerevisterol was found to be a delicate tyrosinase inhibitor, but the only one to exhibit activity against acne causing bacterium *P. acnes*. Additionally, *in vitro* wound healing assay indicated the capability of cerevisterol in promoting dermal fibroblast cell proliferation and migration. These results suggest that microfungi could be a promising candidate for the environmentally friendly production of skin caring agents, particularly in anti-ageing and regenerative formulations.

## Acknowledgements

Professor Huong Le helped with the proofreading of the manuscript; Associate Professor Huong Doan and Doctor Chinh Luu helped to correct and interpret the chemical spectral data.

## Funding

This work was financially supported by the Vietnam Academy of Science and Technology under the grant THTETN.02/24-25. The grant financially supported cosmeceutical assays and related studies on isolation and chemical elucidation of compounds from fungal strains *Penicillium brefeldianum* CL6 and *Talaromyces* sp. S3-Rt-N3.

## Ethical aspects and conflict of interest

I, as the corresponding author, declare that the results/data/figures in this manuscript are original, and have not been published elsewhere. All research was conducted to the highest ethical standards. All authors are involved in the work. Authors and co-authors reviewed and ensured the accuracy and validity of all the results. All authors declare that they have no conflicts of interest.

## References

- Agrawal S, Adholeya A, Barrow CJ, Deshmukh SK (2018). Marine fungi: An untapped bioresource for future cosmeceuticals. *Phytochem Lett* 23: 15–20. DOI: 10.1016/j.phytol.2017.11.003.
- Appiah T, Agyare C, Luo Y, Boamah VE, Boakye YD (2020). Antimicrobial and resistance modifying activities of cerivasterol isolated from *Trametes* species. *Curr Bioact Compd* 16(2): 115–123. DOI: 10.2174/1573407214666180813101146.
- Berridge MV, Herst PM, Tan AS (2005). Tetrazolium dyes as tools in cell biology: new insights into their cellular reduction. *Biotechnol Annu Rev* 11: 127–152. DOI: 10.1016/S1387-2656(05)11004-7.
- Chang TS (2009). An updated review of tyrosinase inhibitors. *Int J Mol Sci* 10(6): 2440–2475. DOI: 10.3390/ijms10062440.
- Cialdai F, Risaliti C, Monici M (2022). Role of fibroblasts in wound healing and tissue remodeling on Earth and in space. *Front Bioeng Biotechnol* 10: 958381. DOI: 10.3389/fbioe.2022.958381.
- Corinaldesi C, Barone G, Marcellini F, Dell'Anno A, Danovaro R (2017). Marine microbial-derived molecules and their potential use in cosmeceutical and cosmetic products. *Mar Drugs* 15(4): 118. DOI: 10.3390/md15040118.
- Dorni AC, Amalraj A, Gopi S, Varma K, Anjana SN (2017). Novel cosmeceuticals from plants-An industry guided review. *J Appl Res Med Aromat Plants* 7: 1–26. DOI: 10.1016/j.jarmap.2017.05.003.
- Espinosa-Leal CA, Garcia-Lara S (2019). Current methods for the discovery of new active ingredients from natural products for cosmeceutical applications. *Planta Med* 85(07): 535–551. DOI: 10.1055/a-0857-6633.
- Galasso C, Corinaldesi C, Sansone C (2017). Carotenoids from marine organisms: Biological functions and industrial applications. *Antioxidants* 6(4): 96. DOI: 10.3390/antiox6040096.
- Gao L, Xu X, Yang J (2013). Chemical constituents of the roots of *Rheum officinale*. *Chem Nat Compd* 49: 603–605. DOI: 10.1007/s10600-013-0689-7.
- Görünmek M, Ballık B, Cakmak ZE, Cakmak T (2024). Mycosporine-like amino acids in microalgae and cyanobacteria: Biosynthesis, diversity, and applications in biotechnology. *Algal Res* 80: 103507. DOI: 10.1016/j.algal.2024.103507.
- Khatib S, Nerya O, Musa R, Shmuel M, Tamir S, Vaya J (2005). Chalcones as potent tyrosinase inhibitors: the importance of a 2, 4-substituted resorcinol moiety. *Bioorg Med Chem* 13(2): 433–441. DOI: 10.1016/j.bmc.2004.10.010.
- Kligman D (2000). Cosmeceuticals. *Dermatol Clin* 18(4): 609–615. DOI: 10.1016/j.bmc.2004.10.010.
- Kogej T, Gostinčar C, Volkmann M, Gorbushina AA, Gunde-Cimerman N (2006). Mycosporines in extremophilic fungi—novel complementary osmolytes? *Environ Chem* 3(2): 105–110. DOI: 10.1071/EN06012.
- Krzyczkowski W, Malinowska E, Suchocki P, Kleps J, Olejnik M, Herold F (2009). Isolation and quantitative determination of ergosterol peroxide in various edible mushroom species. *Food Chem* 113(1): 351–355. DOI: 10.1016/j.foodchem.2008.06.075.
- Li X, Kim MK, Lee U, Kim SK, Kang JS, Choi HD, Son BW (2005). Myrothenones A and B, cyclopentenone derivatives with tyrosinase inhibitory activity from the marine-derived fungus *Myrothecium* sp. *Chem Pharm Bull* 53(4): 453–455. DOI: 10.1248/cpb.53.453.
- Liang CC, Park AY, Guan JL (2007). *In vitro* scratch assay: a convenient and inexpensive method for analysis of cell migration *in vitro*. *Nat Protoc* 2(2): 329–333. DOI: 10.1038/nprot.2007.30.
- Libkind D, Moline M, van Broock M (2011). Production of the UVB-absorbing compound mycosporine-glutaminol-glucoside by *Xanthophyllomyces dendrorhous* (*Phaffia rhodozyma*). *FEMS Yeast Res* 11(1): 52–59. DOI: 10.1111/j.1567-1364.2010.00688.x.
- Lim JY, Ishiguro K, Kubo L (1999). Tyrosinase inhibitory p-coumaric acid from Ginseng leaves. *Phytother Res* 13(5): 371–375. DOI: 10.1002/(sici)1099-1573(199908/09)13:5<371::aid-ptr453>3.0.co;2-l.
- Liu P, Yang Y, Zhou Z, Zhang X, Liu X, Li J (2024). Mitochondrial targeted modification and anticancer mechanism of natural product ergosterol peroxide. *Bioorg Chem* 151: 107688. DOI: 10.1016/j.bioorg.2024.107688.
- Majhi S, Das D (2021). Chemical derivatization of natural products: Semisynthesis and pharmacological aspects-A decade update. *Tetrahedron* 78: 131801. DOI: 10.1016/j.tet.2020.131801.
- Moliné M, Arbeloa EM, Flores MR, Libkind D, Fariás ME, Bertolotti SG, et al. (2011). UVB photoprotective role of mycosporines in yeast: photostability and antioxidant activity of mycosporine-glutaminol-glucoside. *Radiat Res* 175(1): 44–50. DOI: 10.1667/rr2245.1.
- Myers S, Navsaria H, Ojeh N (2014). Skin engineering and keratinocyte stem cell therapy. In: Van Blitterswijk CA, De Boer J (Eds). *Tissue Engineering*. Academic Press, pp. 497–528.
- Nadhilah D, Andriani A, Agustriana E, Nuryana I, Mubarik NR, Dewi KS, et al. (2023). Co-catalysis of melanin degradation by laccase-manganese peroxidase complex from *Trametes hirsuta* OK271075 for application in whitening cosmetics. *Biocatal Biotransfor* 42(2): 273–285. DOI: 10.1080/10242422.2023.2188995.
- Nosanchuk JD, Stark RE, Casadevall A (2015). Fungal melanin: what do we know about structure? *Front Microbiol* 6: 1463. DOI: 10.3389/fmicb.2015.01463.
- Ola AR, Metboki G, Lay CS, Sugi Y, Rozari PD, Darmakusuma D, Hakim EH (2019). Single production of kojic acid by *Aspergillus flavus* and the revision of flufuran. *Molecules* 24(22): 4200. DOI: 10.3390/molecules24224200.
- Orellana EA, Kasinski AL (2016). Sulforhodamine B (SRB) assay in cell culture to investigate cell proliferation. *Bio-Protoc* 6(21): e1984. DOI: 10.21769/BioProtoc.1984.
- Palama TL, Khatib A, Choi YH, Payet B, Fock I, Verpoorte R, Kodja H (2009). Metabolic changes in different developmental stages of *Vanilla planifolia* pods. *J Agric Food Chem* 57(17): 7651–7658. DOI: 10.1021/jf901508f.
- Peña OA, Martin P (2024). Cellular and molecular mechanisms of skin wound healing. *Nat Rev Mol Cell Biol* 25(8): 599–616. DOI: 10.1038/s41580-024-00715-1.
- Pisano L, Turco M, Supuran CT (2024). Chapter Nine – Biomedical applications of tyrosinases and tyrosinase inhibitors. In: Supuran CT (Ed.). *Tyrosinase*. London: Elsevier, pp. 261–280.
- Pretsch A, Nagl M, Schwendinger K, Kreiseder B, Wiederstein M, Pretsch D, et al. (2014). Antimicrobial and anti-inflammatory activities of endophytic fungi *Talaromyces wortmannii* extracts against acne-inducing bacteria. *PloS One* 9(6): e97929. DOI: 10.1371/journal.pone.0097929.
- Qi S, Guo L, Liang J, Wang K, Liao Q, He S, et al. (2024). A new strategy for the treatment of Parkinson's disease: Discovery and bio-evaluation of the first central-targeting tyrosinase inhibitor. *Bioorg Chem* 150: 107612. DOI: 10.1016/j.bioorg.2024.107612.
- Reed RE (1962). The definition of “cosmeceuticals”. *J Soc Cosmet Chem* 13: 103–106.
- Sanjeewa KKA, Kim EA, Son KT, Jeon YT (2016). Bioactive properties and potentials cosmeceutical applications of phlorotannins isolated from brown seaweeds: A review.

- J Photochem Photobiol B 162: 100–105. DOI: 10.1016/j.jphotobiol.2016.06.027.
- Schneider CA, Rasband WS, Eliceiri KW (2012). NIH Image to ImageJ: 25 years of image analysis. *Nat Methods* 9(7): 671–675. DOI: 10.1038/nmeth.2089.
- Sharma K, Kumar S, Chand K, Kathuria A, Gupta A, Jain R (2011). An update on natural occurrence and biological activity of chromones. *Curr Med Chem* 18(25): 3825–3852. DOI: 10.2174/092986711803414359.
- Singh A, Singh D, Kharwar RN, White JF, Gond SK (2021). Fungal endophytes as efficient sources of plant-derived bioactive compounds and their prospective applications in natural product drug discovery: Insights, avenues, and challenges. *Microorganisms* 9(1): 197. DOI: 10.3390/microorganisms9010197.
- Vanden Berghe DA, Vlietinck AJ (1991). Screening methods for antibacterial and antiviral agents from higher plants. In: Hostettmann K (Ed.). *Methods in Plant Biochemistry*. London: Academic Press, pp. 47–69.
- Visagie CM, Houbraken J, Frisvad JC, Hong SB, Klaasen C HW, Perrone G, et al. (2014). Identification and nomenclature of the genus *Penicillium*. *Stud Mycol* 78: 343–371. DOI: 10.1016/j.simyco.2014.09.001.
- Volkman M, Gorbushina AA (2006). A broadly applicable method for extraction and characterization of mycosporines and mycosporine-like amino acids of terrestrial, marine and freshwater origin. *FEMS Microbiol Lett* 255(2): 286–295. DOI: 10.1111/j.1574-6968.2006.00088.x.
- Wang Y, Xiong B, Xing S, Chen Y, Liao Q, et al. (2023). Medicinal prospects of targeting tyrosinase: A feature review. *Curr Med Chem* 30(23): 2638–2671. DOI: 10.2174/0929867329666220915123714.
- Wong HJ, Mohamad-Fauzi N, Rizman-Idid M, Convey P, Alias SA (2019). Protective mechanisms and responses of micro-fungi towards ultraviolet-induced cellular damage. *Polar Sci* 20(Part 1): 19–34. DOI: 10.1016/j.polar.2018.10.001.
- White TJ, Bruns TD, Lee SB, Taylor JW (1990). Amplification and direct sequencing of fungal ribosomal RNA genes for phylogenetics. In: Innis MA, Gelfand DH, Sninsky JJ, White TJ (Eds). *PCR Protocols: A Guide to Methods and Applications*. New York: Academic Press, pp. 315–322.
- Wu B, Oesker V, Wiese J, Schmaljohann R, Imhoff JF (2014). Two new antibiotic pyridones produced by a marine fungus, *Trichoderma* sp. strain MF106. *Mar Drugs* 12(3): 1208–1219. DOI: 10.3390/md12031208.
- Wu B, Wu X, Sun M, Li M (2013). Two novel tyrosinase inhibitory sesquiterpenes induced by CuCl<sub>2</sub> from a marine-derived fungus *Pestalotiopsis* sp. Z233. *Mar Drugs* 11(8): 2713–2721. DOI: 10.3390/md11082713.
- Xiong HY, Fei DQ, Zhou JS, Yang CJ, Ma GL (2009). Steroids and other constituents from the mushroom *Armillaria lueo-virens*. *Chem Nat Compd* 45: 759–761. DOI: 10.1007/s10600-009-9456-1.
- Ye K, Ai HL, Liu JK (2021). Identification and bioactivities of secondary metabolites derived from endophytic fungi isolated from ethnomedicinal plants of Tujia in Hubei province: a review. *Nat Prod Bioprospecting* 11(2): 185–205. DOI: 10.1007/s13659-020-00295-5.
- Yilmaz N, Visagie C M, Houbraken J, Frisvad JC, Samson RA (2014). Polyphasic taxonomy of the genus *Talaromyces*. *Stud Mycol* 78: 175–341. DOI: 10.1016/j.simyco.2014.08.001.
- Zhang X, Kang X, Jin L, Bai J, Liu W, Wang Z (2018). Stimulation of wound healing using bioinspired hydrogels with basic fibroblast growth factor (bFGF). *Int J Nanomedicine* 13: 3897. DOI: 10.2147/IJN.S168998.
- Zhang ZY, Jin B, Kelly JM (2007). Production of lactic acid from renewable materials by *Rhizopus* fungi. *Biochem Eng J* 35(3): 251–263. DOI: 10.1016/j.bej.2007.01.028.
- Zhou X, Brown BA, Siegel AP, El Masry MS, Zeng X, Song W, et al. (2020). Exosome-mediated crosstalk between keratinocytes and macrophages in cutaneous wound healing. *ACS Nano* 14(10): 12732–12748. DOI: 10.1021/acsnano.0c03064.
- Zhu H, Qu F, Zhu LH (1993). Isolation of genomic DNAs from plants, fungi and bacteria using benzyl chloride. *Nucleic Acids Res* 21(22): 5279–2580. DOI: 10.1093/nar/21.22.5279.